ACS APPLIED MATERIALS & INTERFACES

www.acsami.org

Research Article

Light-Mediated Shape Transformation of a Self-Rolling Nanocomposite Hydrogel Tube

Hongyu Guo,* Qian Zhang, Wei Liu, and Zhihong Nie

Cite This: *ACS Appl. Mater. Interfaces* 2020, 12, 13521−13528

Read Online

ACCESS | Metrics & More | Article Recommendations | Supporting Information

ABSTRACT: Self-rolling of a planar hydrogel sheet represents an advanced approach for fabricating a tubular construct, which is of significant interest in biomedicine. However, the self-rolling tube is usually lacking in remote controllability and requires a relatively tedious fabrication procedure. Herein, we present an easy and controllable approach for fabricating self-rolling tubes that can respond to both magnetic field and light. With the introduction of magnetic nanorods in a hydrogel precursor, a strain gradient is created across the thickness of the formed hydrogel sheet during the photopolymerization process. After the removal of the strain constraint, the nanocomposite sheet rolls up spontaneously. The self-rolling scenario of the sheet can be tuned by varying the sheet geometry and the magnetic nanorod concentration in the hydrogel precursor. The nanocomposite hydrogel tube translates in the presence of a magnetic field and produces heat upon a near-infrared (NIR) light illumination by virtue of the magnetic and photo-thermal properties of the magnetic nanorods. The self-rolling tube either opens up or expands its diameter under NIR light irradiation depending on the number of rolls in the tube. With the use of a thermo-responsive hydrogel material, we demonstrate the magnetically guided motion of the chemical-bearing nanocomposite hydrogel tube and its controlled chemical release through its light-mediated deformation. The approach reported herein is expected to be applicable to other self-rolling polymer-based dry materials, and the nanocomposite hydrogel tube presented in this work may find potential applications in soft robot and controlled release of drug.

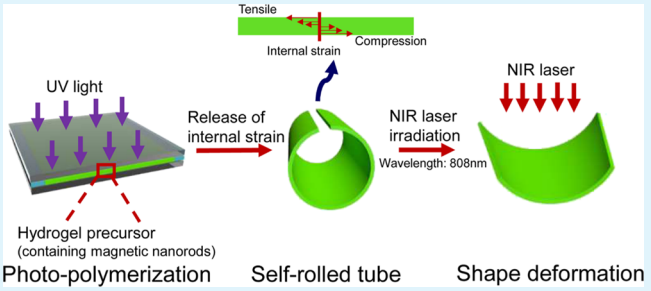

KEYWORDS: *responsive, residual strain, photopolymerization, near-infrared light, composite material, shape changing*

INTRODUCTION

Natural living things have adapted to change their shapes for survival in response to environmental variations.[1] Examples include the helical twisting of a seed pod,[2] the opening of a pine cone,[3] the snap-buckling of a Venus flytrap,[4] and so forth as a result of the humidity change[2,3] or a mechanical touch.[4] The underlying mechanism of the shape switches among these plant organs is due to the layered structure in the active organs in which swelling behaviors differ in different layers in the presence of environmental stimuli.[2,3] Inspired by this self-shaping mechanism, researchers from around the globe have devoted remarkable efforts over the past decades to design shape-changing systems with the desire of benefiting humankind.[5−35] The application potentials of the shape-morphing systems can be found in a wide range of research fields, such as in tissue engineering,[36−39] soft robot,[40−50] microsurgery,[51,52] microfluidics,[53,54] drug/cell delivery,[55−57] metamaterial,[58,59] among many others.[12,16,17]

Among the various three-dimensional constructs, the tubular structure is of particular interest as it resembles a blood vessel.[60] The tubular construct has been investigated as a cell scaffold,[37−39,61] actuator,[54,60,62] molecular/cellular release,[57,63,64] cell confinement media,[36,65] and so forth. The self-rolling of a planar sheet represents a remarkably attractive method to form a tubular construct due to its low cost, easiness to be realized, compatibility with a lithographic patterning technique, and easiness to be endowed with functionality.[12] Typically, the rolling-up of a planar sheet can be achieved by generating a layered structure with dissimilar properties among individual layers, such as lattice mismatch, differential thermal expansion, or swelling.[66] For example, Stoychev et al. fabricated a polymer-based bilayer sheet in which the swelling property varied between the two layers.[66] Upon the activation of the stimulus (water), the differential expansion between the two layers resulted in the self-rolling of the bilayer sheet. In another example, Chun et al. fabricated a semiconductor membrane with a bilayer form.[67] Due to the epitaxial mismatch between the two layers, the strain energy was stored in the membrane during its preparation, which caused the rolling-up

Received: December 23, 2019
Accepted: February 25, 2020
Published: February 25, 2020

https://dx.doi.org/10.1021/acsami.9b23195
ACS Appl. Mater. Interfaces 2020, 12, 13521−13528

of the membrane when the constraint of the strain was removed. However, most of the rolled-up tubes reported before are lacking in their capability for remote control, which can be beneficial for the light-controlled release of cell/drug.[57] In addition, the realization of self-rolling through the fabrication of a layered sheet is a relatively tedious process and is desired to be improved.

Herein we present an easy and controllable approach to fabricate self-rolling nanocomposite hydrogel tubes and study their light-guided shape deformations (Figure 1). Magnetic

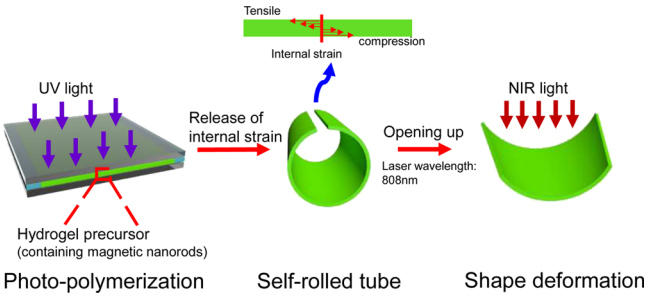

Figure 1. Schematic illustration of the photopolymerization of a hydrogel precursor, self-rolling of the hydrogel sheet, and shape deformation of the nanocomposite hydrogel tube under an NIR light irradiation.

nanorods were introduced in the poly(*N*-isopropylacrylamide) hydrogel precursor, which was then subjected to an ultraviolet (UV) polymerization. Due to the UV light intensity decay resulting from the UV light extinction of magnetic nanorods, a strain gradient was generated across the thickness of the formed hydrogel sheet during the photopolymerization process. After the removal of the strain constraint from the hydrogel fabrication mold, the nanocomposite sheet deformed spontaneously. The deformation scenario of the sheet, such as bending, helical twisting, and single and double-rolling, can be tuned by varying the sheet geometry and nanorod concentration in the hydrogel precursor. The nanocomposite hydrogel tube translates in the presence of a magnetic field and produces heat upon a near-infrared (NIR) light illumination by virtue of the magnetic and photo-thermal properties of the magnetic nanorods. The self-rolling tube either opens up or expands its diameter under NIR light irradiation depending on the number of rolls in the tube. With the use of a thermo-responsive hydrogel material, we demonstrate the magnetically guided motion of the chemical-bearing nanocomposite hydrogel tube and its controlled chemical release through its light-mediated deformation. The approach reported herein is expected to be applicable to other self-rolling polymer-based materials, and the nanocomposite hydrogel tube presented in this work may find potential applications in soft robot and controlled release of drug.

EXPERIMENTAL SECTION

Materials. All chemicals were purchased from Sigma-Aldrich and were used without further treatment. Chemicals used were as follows: *N*-isopropylacrylamide (NIPAm, monomer), *N*,*N*′-methylenebis(acrylamide) (BIS, cross linker), and 2,2′-azobis(2-methylpropionamidine)dihydrochloride (photo-initiator, V50). Polyvinylpyrrolidone (PVP, MW 29,000), tetraethyl orthosilicate (TEOS), anhydrous ethanol, ammonium hydroxide (25.0−28.0%), anhydrous ferric chloride ($FeCl_3$), hydrochloric acid (37.5%), and diethylene glycol (DEG). Milli-Q water with a resistance of 18.2 MΩ·cm was used throughout the experiments.

Synthesis of the Magnetic Nanorod. A modified approach based on the previous work was used to synthesize a large quantity of magnetic nanorods.[68] The first step was to synthesize rod-like FeOOH. Typically, 50 μL hydrochloric acid was added to 80 mL water in a 100 mL round-bottom flask with a magnetic stirring bar. Following that, 7.776 g anhydrous $FeCl_3$ was added and stirred to dissolve on an ice bed. The solution was heated to 98 °C with a condenser attached. After 16 h, the flask was cooled down in an ice bath. The solution was then centrifuged at 10,000 rpm for 10 min and washed by using water four times. Finally, the rod-shaped FeOOH was dried under vacuum at room temperature. Next, PVP was coated onto FeOOH rods. PVP (9.67 g) was dissolved in 400 mL water in a round-bottom flask. To this, 200 mg dried FeOOH rods were added. The solution was subject to sonication to disperse the FeOOH rods. Finally, the solution was mechanically stirred overnight for PVP coating. After PVP coating, the solution was centrifuged at 10,000 rpm for 10 min and washed by using water four times and then by using ethanol two times. After washing, these PVP-coated FeOOH rods were re-dispersed in 350 mL ethanol. Under mechanical stirring, 31.5 mL ammonium hydroxide was added, followed by the addition of 833 μL TEOS. The solution was mechanically stirred for 20 h to coat silica on FeOOH rods. After silica coating, the solution was centrifuged at 10,000 rpm for 10 min and washed by using water six times. The silica-coated FeOOH rods were then re-dispersed in 80 mL DEG. The DEG solution containing silica-coated FeOOH rods was transferred to a 100 mL autoclave vessel and was subject to 220 °C for 24 h in air in an oven. At this step, the silica-coated FeOOH rods were converted to silica-coated magnetic nanorods. After the conversion, the DEG solution was diluted with ethanol and was subject to centrifugation at 10,000 rpm for 10 min and washed using water five times. Finally, the silica-coated magnetic nanorod was dried under vacuum at room temperature for two days.

Synthesis of the Nanocomposite Hydrogel Sheet. The nanocomposite hydrogel sheet was fabricated by photopolymerization. Typically, 0.045 g magnetic nanorod was dispersed in 1 mL water under sonication. Following that, 0.113 g NIPAm monomer, 0.008 g BIS cross linker, and 0.002 g photo initiator (V50) were added to the solution. After dissolution, this hydrogel precursor was injected into a pre-made mold made of two glass slides and a spacer. The hydrogel precursor was subject to UV irradiation at 365 nm wavelength for 45 min. After fabrication, one glass slide was carefully peeled off, leaving the hybrid hydrogel physically attached to the other piece of glass slide. Hydrogel pieces with certain length and width were cut out of the as-fabricated hydrogel sheet with a razor blade for the self-rolling study.

Self-Rolling of the Nanocomposite Hydrogel Sheet. The as-fabricated hydrogel sheet, which was physically attached to the glass slide, was cut into pieces with certain length and width. After releasing the hydrogel pieces from the glass slide into water, the hydrogel sheets rolled up spontaneously due to the release of the residual strain generated during the fabrication of the composite sheet.

Light-Triggered Shape Transformation of the Nanocomposite Hydrogel Tube. An 808 nm laser (MDL-N-808, Changchun New Industries Optoelectronics Technology Co. Ltd., China) was used as the light source. During the experiments, the nanocomposite hydrogel tube was immersed in 20 mL water in a glass Petri dish.

Chemical Release Study by Using the Nanocomposite Hydrogel Tube. Before loading the dye, the self-rolling tube was kept in water. Then, the self-rolling tube was immersed in a rhodamine B aqueous solution of 1 mg/mL for 1 min for the dye to diffuse into the tubular lumen and into the hydrogel matrix. Then the rhodamine-loaded tube was taken out and the water on the tube's surfaces was carefully wiped off by using a paper tissue. After that, the rhodamine B-loaded tube was immersed in 20 mL deionized water in a glass Petri dish. Thereafter, the tube was irradiated by laser. The expansion of the tubular lumen and the heat generated in the hydrogel matrix accelerated the release of rhodamine B from the tube into water. After switching off the laser, the tube contracted, resulting in

https://dx.doi.org/10.1021/acsami.9b23195
ACS Appl. Mater. Interfaces 2020, 12, 13521−13528

further release of rhodamine B. The fluorescence of the surrounding water was measured and the accumulated amount of released rhodamine B was calculated through the standard fluorescence curve of rhodamine B.

UV−Vis−NIR Measurement of the Magnetic Nanorod. The optical property of the magnetic nanorod aqueous solution was characterized by measuring its light extinction using UV−Vis−NIR spectroscopy (Lambda 40 UV/VIS Spectrometer, PerkinElmer, USA). Magnetic nanorod aqueous solutions with different weight percentages of the magnetic nanorod were prepared, and their UV−Vis−NIR spectra were measured. The UV−Vis−NIR spectra were taken at a slit width of 1 nm, scanning speed of 480 nm/min, and data interval of 1 nm.

SEM of the Magnetic Nanorod and Nanocomposite Hydrogel Sheet. For the magnetic nanorod characterization, a drop of its aqueous solution was dried on a silicon wafer, and the dried sample was imaged by using scanning electron microscopy (SEM) (XL Series-30, Philips, USA). For the nanocomposite hydrogel sheet characterization, the hydrogel sheet was first freeze-dried and then coated with gold (JFC-1200 Fine Coater, Japan). Following that, SEM was used to characterize its structure.

Swelling of the Nanocomposite Hydrogel Sheet. The swelling property of the nanocomposite hydrogel sheet was characterized by using the swelling ratio of the composite sheet, which was measured gravimetrically after wiping off the excess water on the hydrogel's surface with a piece of Kimwipe in the temperature range from 18 to 37 °C. The nanocomposite hydrogel sheet was incubated in a water bath for at least 24 h at each temperature. The swelling ratio of the composite sheet was calculated by using the following formula

$$\text{Swelling ratio} = W_s/W_d$$

where W_s was the weight of the swollen hydrogel at the particular temperature and W_d was the dry weight of the hydrogel.

Photothermal Property of the Nanocomposite Hydrogel Tube. The photothermal property of the nanocomposite hydrogel tube was studied by the photothermal imaging technique. Briefly, the nanocomposite hydrogel tube was immersed in 20 mL water in a glass Petri dish and was irradiated with an 808 nm laser at a power of 5 W (laser power density: 2.83 W/cm^2) for 1 min and then the laser was shut off. During the process, the surface temperature of the composite hydrogel tube was monitored by using an FLIR SC300 infrared camera (FLIR, Arlington, VA). Real-time thermal images were captured with the frame rate at 60 Hz and analyzed by the FLIR Examiner software.

RESULTS AND DISCUSSION

Fabrication of the Magnetic Nanorod and Nanocomposite Hydrogel Sheet. A magnetic nanorod with a length of 800 nm and a diameter of 70 nm was successfully synthesized (Figure 2a,b) and introduced into the hydrogel sheet (Figure 2c,d). The magnetic nanorod aqueous solution has light extinction in a broad wavelength range. The light extinction of the nanorod solution can be tuned by changing the nanorod concentration. For example, the light extinction increased from 0.1 to 0.2 at the light wavelength of 808 nm when the nanorod concentration was increased from 0.1 to 0.2 mg/mL.

Self-Rolling of the Nanocomposite Hydrogel Sheet. The nanocomposite hydrogel sheet spontaneously rolled up when removed from the glass substrate probably due to the release of the internal strain in the hydrogel sheet that was generated in the photopolymerization process. As studied by Zhao et al., the introduction of a photo-absorber (a chemical dye in their case) in a polymer resin precursor resulted in an UV light intensity decay as the light penetrated through the resin during the photopolymerization process.[69] This led to an

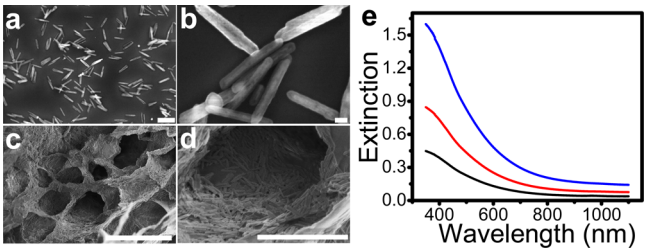

Figure 2. (a,b) SEM of the as-synthesized magnetic nanorods. The magnetic nanorod has a length of around 800 nm and a diameter of 70 nm; (c,d) SEM of the nanocomposite hydrogel sheet. The magnetic nanorods were successfully introduced in the hydrogel sheet; (e) light extinction property of the aqueous solution of magnetic nanorods with different nanorod concentrations. The black, red, and blue curves suggest a nanorod concentration of 0.05, 0.1, and 0.2 mg/mL, respectively. Scale bar is 1 μm in (a), 100 nm in (b), 10 μm in (c), and 3 μm in (d).

internal strain in the polymerized resin, resulting in its bending deformation after removal of the strain constraint. In our case, the magnetic nanorod introduced in the hydrogel precursor served as the photo-absorber due to its light extinction property. Therefore, a differential volumetric shrinkage along the thickness direction of the polymerized hydrogel sheet was realized during the photopolymerization process, which created a strain gradient within the sheet. By removing the strain constraint (the substrate), the nanocomposite hydrogel sheet bent or rolled up autonomously without the presence of an external stimulus. As suggested by the previous work on the bending deformation of a thin film with a bilayer structure, the length and width of the thin film affect its bending/rolling scenario.[66,67] We therefore systematically investigated the effect of the length and width of the nanocomposite hydrogel sheet on its deformation and constructed a deformation diagram (Figure 3a). The magnetic nanorod content is 4.5 wt % in the hydrogel precursor with respect to its water content. This hydrogel precursor is used to fabricate the nanocomposite hydrogel sheet that has deformation behaviors, as shown in Figure 3. As seen from Figure 3, the deformation of the nanocomposite hydrogel sheet could span from bending to helical twisting and to single and double rolling by altering its length and width (Figure 3a,c−f). For example, when the sheet width was fixed at 0.2 cm, the deformation of the nanocomposite hydrogel sheet changed from helical twisting to single rolling and to double rolling when the sheet length was increased from 0.3 to 0.5 and to 1 cm, respectively (Figure 3a). With a mechanical perturbation, the same self-rolled tube could have different forms, such as a single tube with different rolling axes, twin tubes, helical tube, and so forth (Figure S1). By changing the amount of magnetic nanorods introduced in the hydrogel precursor, we varied the deformation diagram of the composite hydrogel sheet. For example, the parametric domain for producing a doubly rolled tube narrowed when decreasing the amount of magnetic nanorods in the hydrogel precursor from 4.5 to 2 wt % (Figure S2). We noted that the hydrogel sheet took on a planar shape when the magnetic nanorod was not introduced in the hydrogel precursor due to the lack of a significant strain gradient in the sheet. The thickness of the nanocomposite hydrogel sheet is found to have a remarkable influence on its rolling behavior (Figure 3b). For example, a sheet with a length of 1 cm and a width of 0.2 cm rolls up to form a tube when its thickness is 250 μm, while

https://dx.doi.org/10.1021/acsami.9b23195
ACS Appl. Mater. Interfaces 2020, 12, 13521−13528

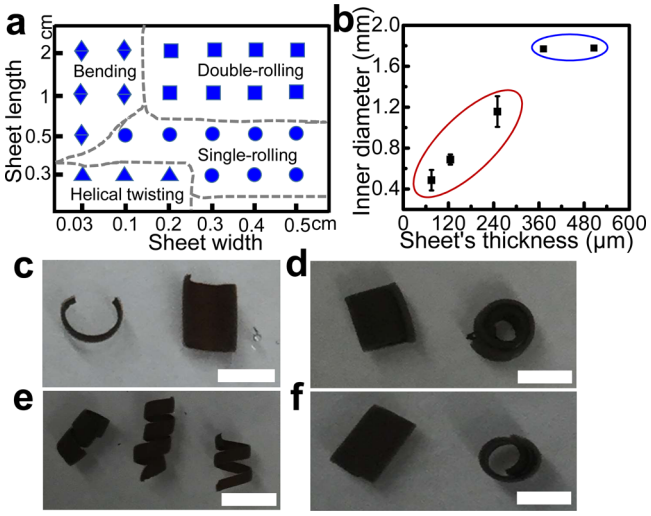

Figure 3. Shape deformation of the nanocomposite hydrogel sheet with varied sheet width, length, and thickness. (a) Deformation diagram summarizing the sheet's geometric parameters for each shape deformation scenario as shown in (c–f); (b) effect of sheet's thickness on its rolling behavior; (c) bending deformation; (d) double-rolling deformation; (e) helical twisting deformation; (f) single-rolling deformation. The thickness of the nanocomposite hydrogel sheet is 125 μm in (a,c–f). The sheet in (b) has a length of 1 cm and a width of 0.2 cm. The studied sheet's thickness in (b) is 75, 125, 250, 375, and 500 μm. The red elliptical curve in (b) indicates that the sheet rolls up to form a tube, while the blue elliptical curve suggests that the sheet remains flat at the designated sheet's thickness. The magnetic nanorod content in the hydrogel precursor is 4.5 wt % with respect to the water content in it. The images in c–f were taken by the camera from an iPad. Scale bar: 0.5 cm.

it remains flat when its thickness is 375 μm. For the sheet that rolls up to form a tube, the inner diameter of the self-rolling tube increases with the increase of the sheet's thickness (Figure 3b). The bending and rolling behavior of the nanocomposite hydrogel sheet can be qualitatively understood by using the theoretical model developed for the photopolymerized resin system.[69] The model is based on the beam theory. Based on this model, the bending curvature of the sheet depends on the distribution of stress and Young's modulus in the sheet and on the sheet's thickness. The model indicates that with the increase of the sheet's thickness, its bending curvature decreases. This corresponds well to the bending behavior of the nanocomposite hydrogel sheet reported herein since the inner diameter of the self-rolling nanocomposite hydrogel tube increases (i.e., the bending curvature decreases) by increasing the thickness of the nanocomposite hydrogel sheet (Figure 3b). The model also suggests that the sheet remains flat without the presence of the stress gradient in it. This agrees well with the bending behavior of the hydrogel sheet in that the hydrogel sheet is flat when magnetic nanorods are not present in the hydrogel precursor in the photopolymerization process, which results in the lack of an appreciable stress gradient in the sheet. By altering the original shape of the nanocomposite hydrogel sheet, we obtained different three-dimensional structures upon removal of the strain constraint (Figure S3). For instance, a dumbbell-like hydrogel sheet transformed to a nose-like structure upon release of the internal strain in the sheet (Figure S3a).

Swelling and Photothermal Property of the Nanocomposite Hydrogel. The hydrogel material (PNIPAm hydrogel) used in the present work is a well-known thermo-responsive hydrogel whose swelling extent decreases with an increasing temperature.[60,70] A similar trend between the swelling extent and the temperature was found for the nanocomposite hydrogel sheet reported here. The swelling extent of the nanocomposite hydrogel sheet decreased monotonically with the increase of the temperature and finally reached a swelling state in which the swelling extent did not change appreciably by further increasing the temperature (Figure S4). The surface temperature of the nanocomposite hydrogel tube was increased under the laser irradiation as a result of the heat generated by the magnetic nanorods inside the hydrogel via their photothermal effect (Figure 4). The

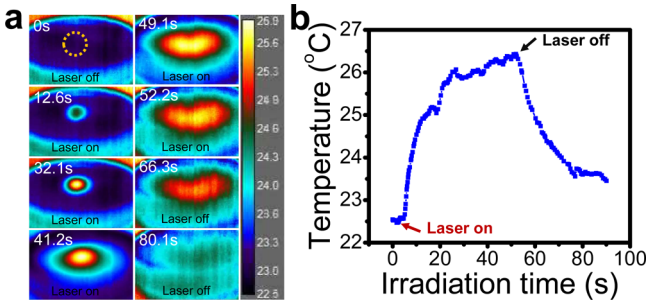

Figure 4. (a) Photothermal images of the nanocomposite hydrogel tube system during the laser on-and-off process as a function of the irradiation time (in seconds); (b) surface temperature evolution of the nanocomposite hydrogel tube as a function of the laser irradiation time corresponding to data in (a). The color legend shown on the right-hand side of (a) suggests the temperature scale (in °C). The numbers shown on the top left corner of the photothermal images in (a) indicate the time in seconds (s) when the photothermal image was taken during the laser on-and-off process. The yellow dashed circle in the photothermal image taken at 0 s in (a) indicates the position of the nanocomposite hydrogel tube in the water-containing glass Petri dish before the laser irradiation.

temperature profile of the nanocomposite hydrogel tube system evolved during the laser on-and-off process (Figure 4a). With the increase of the laser irradiation time, the area that has a larger temperature than the ambience enlarged. The shape of the temperature profile was altered due to the shape deformation of the nanocomposite hydrogel tube that occurred at about 50 s while the laser irradiation is kept on. The surface temperature of the nanocomposite hydrogel tube immersed in 20 mL water increased from the ambience temperature of 22.5 °C to 26.4 °C after the nanocomposite hydrogel tube was irradiated for 52 s by laser, and it gradually decreased to the ambience temperature after the laser was shut off (Figure 4a,b). We note that the surface temperature of the nanocomposite hydrogel tube reached 40 °C by irradiating the tube in air under the same laser power density and irradiation time as that used for irradiating the tube in water. The temperature around the photothermal-converting magnetic nanorods inside the hydrogel network is expected to be high, which exceeds the LCST (lower critical solution temperature)of the PNIPAm hydrogel and results in its deformation, although the surface temperature (26.4 °C) of the tube measured in this study is lower than PNIPAm's LCST. It remains challenging to measure the temperature inside the hydrogel network for our system for the time being.

Shape Transformation of the Nanocomposite Hydrogel Tube under Laser Irradiation. The self-rolled nano-

https://dx.doi.org/10.1021/acsami.9b23195
ACS Appl. Mater. Interfaces 2020, 12, 13521−13528

composite hydrogel tube transformed its shape under an NIR laser irradiation (Figure 5). For example, a single-roll tube

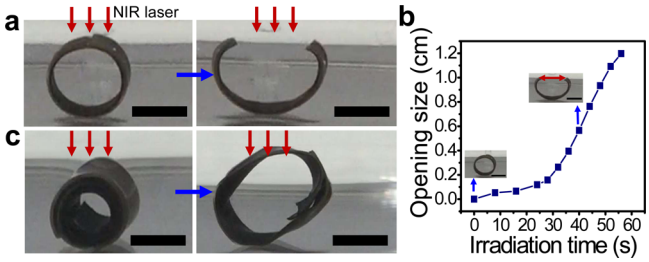

Figure 5. Shape deformation of self-rolling nanocomposite hydrogel tubes under laser irradiation. (a) Shape deformation of a single-roll tube. The single-roll tube opens up upon laser irradiation; (b) opening size of the single-roll tube as a function of the laser irradiation time. The opening size of the single-roll tube increases with the increase of the irradiation time. The red double arrow in the inset image of the graph indicates the opening size of the tube; (c) shape deformation of a double-roll tube. The tubular diameter of the double-roll tube enlarges under laser irradiation. The thickness of the composite hydrogel sheet is 125 μm. The images shown in the figure were taken by the camera from an iPad. Scale bar: 0.3 cm.

opened up upon the laser illumination and its opening size could be controlled by the laser irradiation time (Figure 5a,b and supporting video 1). For example, the opening size of the single-roll tube increased from 0 to 1 cm after the single-roll tube was irradiated for 50 s (Figure 5b). For the double-roll tube, its tubular diameter enlarged under the laser irradiation (Figure 5c and supporting video 2). The shape transformations were realized through the combination of the photo-thermal property of the magnetic nanorods and the thermo-responsiveness of the hydrogel matrix. When light was cast on the self-rolled hydrogel tube, heat was generated by the magnetic nanorods via the photo-thermal effect, as confirmed by the gradual increase of the composite tube's surface temperature (Figure 4). Since the swelling experiment indicated that the composite hydrogel gradually lost water with a step-wise increase of the temperature (Figure S4), the temperature increase of the tube's outer surface that was irradiated by laser caused the shrinkage of the outer surface. It was believed that the shrinkage was different in the thickness direction of the nanocomposite hydrogel due to the extinction of the NIR light caused by the nanocomposite hydrogel as the NIR light penetrates through it. Therefore, a "bilayer-type" structure with a differential swelling extent among the "layers" was believed to be created along the thickness direction of the homogeneous sheet under the NIR laser irradiation.[70] This differential swelling along the sheet's thickness direction results in the tube's opening-up or expansion in its diameter by competing against the stress gradient inside the as-fabricated sheet that causes its rolling.

We pointed out that the shape deformation of the nanocomposite hydrogel tube was reversible and could be repeated many times. The reversibility of the shape deformation made the self-rolled tube desirable in the controlled release of the drug by its cyclic opening/expansion (when the laser was on) and closing/contraction (when the laser was off). We note that the response of the nanocomposite hydrogel tube toward light is fast (on the order of seconds) and could be enhanced by reducing the thickness of the hydrogel.

Chemical Release Behavior of the Nanocomposite Hydrogel Tube. A double-roll nanocomposite hydrogel tube was used as the chemical carrier, and its chemical release behavior was studied during the laser on-and-off process (Figure 6, see supporting video 3). The double-roll tube was

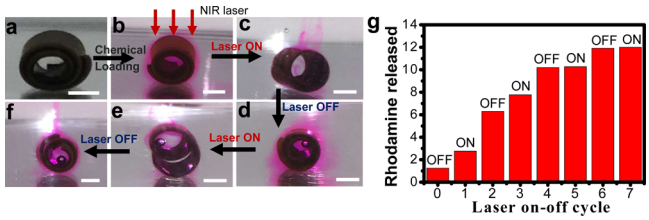

Figure 6. Chemical release behavior of the nanocomposite hydrogel tube during the laser on-and-off process. (a) Double-roll tube used in loading chemical (rhodamine B); (b) double-roll tube loaded with rhodamine B (pink color); (c–f) release of rhodamine B from the tube in the cyclic laser on–off process; (g) accumulated amount of rhodamine B ($\times 10^{-3}$ mg) released from the tube during the laser on–off process. The images in (a–f) were taken by the camera from an iPad. Image (a) was taken in water when the tube was not loaded with the dye. After the tube was loaded with the dye, it was transferred to another container having water in it. Then, images (b–f) were taken during the laser on-and-off process. Scale bar: 0.1 cm.

first loaded with the chemical, rhodamine B, in its tubular lumen and in the hydrogel matrix via a concentration-driven diffusion mechanism (Figure 6a,b). Before laser irradiation, rhodamine B diffused from the hydrogel matrix and from the tubular lumen into water (Figure 6b). Upon laser irradiation, the intense deformation of the tube and the heat generated in the hydrogel matrix significantly accelerated the release of rhodamine B (Figure 6c, supporting video 3). After switching off the laser, the expanded tube contracted and resulted in a further chemical release (Figure 6d, supporting video 3). Through the cyclic laser on–off process (Figure 6c–f), rhodamine B was gradually released from the tube into the surroundings (Figure 6g). By utilizing the magnetic property of the magnetic nanorods, the chemical-loaded tube could be transported to a desired site by using a magnet. After being transported to the target site, the nanocomposite tube was irradiated by an NIR laser, which deformed the tube and released the chemical (see supporting video 4).

CONCLUSIONS

In conclusion, we present an easy and controllable approach to fabricate self-rolled nanocomposite tubes that can respond to both magnetic field and light. By introducing magnetic nanorods in a hydrogel precursor, a strain gradient was created across the thickness of the hydrogel sheet during the photopolymerization process. After the removal of the strain constraint, the nanocomposite hydrogel sheet deformed spontaneously. The deformation scenario of the sheet, such as bending, helical twisting, and single and double rolling, can be tuned by varying the sheet geometry and nanorod concentration in the hydrogel precursor. The nanocomposite hydrogel tube translates in the presence of a magnetic field and produces heat upon a near-infrared (NIR) light illumination by utilizing the magnetic and photo-thermal properties of the magnetic nanorods. The self-rolled tube either opens up or expands its diameter under NIR light irradiation depending on the number of rolls in the tube. With the use of a thermo-responsive poly(*N*-isopropylacrylamide) hydrogel material, we

https://dx.doi.org/10.1021/acsami.9b23195
ACS Appl. Mater. Interfaces 2020, 12, 13521–13528

demonstrated the magnetically guided motion of the chemical-bearing nanocomposite hydrogel tube and its controlled chemical release through its light-mediated deformation. The response of the composite hydrogel tube toward light is fast (on the order of seconds) and could be remarkably enhanced by reducing the thickness of the nanocomposite hydrogel. By using the same fabrication approach, self-rolled tubes could be achieved from other hydrogel monomer materials, such as acrylamide, *N*,*N*-diethylacrylamide, *N*,*N*-dimethylacrylamide, and their combinations. The approach reported herein is also expected to be applicable to other self-rolling polymer-based dry materials. To conclude, the self-rolling nanocomposite hydrogel tube reported here represents an interesting and advanced platform. It has rich scientific phenomena and bears good potentials in a broad range of technological fields, such as in the controlled release of drug, microfluidics, and soft robotics.

■ ASSOCIATED CONTENT

Supporting Information

The Supporting Information is available free of charge at https://pubs.acs.org/doi/10.1021/acsami.9b23195.

Deformation diagram of the nanocomposite hydrogel sheet with a reduced magnetic nanorod loading, shape deformation of a double-rolling tube via mechanical perturbation, shape deformation of nanocomposite hydrogel sheets with different original shapes, swelling of the nanocomposite hydrogel sheet as a function of the water temperature, shape deformation of a single-rolling nanocomposite hydrogel tube under a bulk heating (PDF)

A single-roll tube opened up upon laser illumination (AVI)

Tubular diameter of a double-roll tube enlarged under laser irradiation (AVI)

Double-roll nanocomposite hydrogel tube used as the chemical carrier and its chemical release behavior during the laser on-and-off process (AVI)

Irradiation of the nanocomposite tube after being transported to the target site (AVI)

■ AUTHOR INFORMATION

Corresponding Author

Hongyu Guo − *Jiangxi Key Laboratory for Mass Spectrometry and Instrumentation, East China University of Technology, Nanchang 330013, P. R. China; Department of Chemistry and Biochemistry, University of Maryland, College Park 20742, Maryland, United States;* orcid.org/0000-0002-8488-0898; Email: guohy89@163.com

Authors

Qian Zhang − *Department of Chemistry and Biochemistry, University of Maryland, College Park 20742, Maryland, United States*

Wei Liu − *Jiangxi Key Laboratory for Mass Spectrometry and Instrumentation, East China University of Technology, Nanchang 330013, P. R. China;* orcid.org/0000-0003-0556-2013

Zhihong Nie − *State Key Laboratory of Molecular Engineering of Polymers, Department of Macromolecular Science, Fudan University, Shanghai 200438, P. R. China; Department of Chemistry and Biochemistry, University of Maryland, College Park 20742, Maryland, United States;* orcid.org/0000-0001-9639-905X

Complete contact information is available at: https://pubs.acs.org/10.1021/acsami.9b23195

Notes

The authors declare no competing financial interest.

■ ACKNOWLEDGMENTS

H.G. and W.L. acknowledge the Startup Fund from East China University of Technology (no. DHBK2019259 and no. DHBK2017112, respectively). We also acknowledge the support of the Maryland NanoCenter and its NispLab. The NispLab is supported in part by the NSF as a member of the MRSEC Shared Experimental Facilities.

■ REFERENCES

(1) Burgert, I.; Fratzl, P. Actuation Systems in Plants as Prototypes for Bioinspired Devices. *Philos. Trans. R. Soc., A* **2009**, *367*, 1541−1557.

(2) Armon, S.; Efrati, E.; Kupferman, R.; Sharon, E. Geometry and Mechanics in the Opening of Chiral Seed Pods. *Science* **2011**, *333*, 1726−1730.

(3) Erb, R. M.; Sander, J. S.; Grisch, R.; Studart, A. R. Self-Shaping Composites with Programmable Bioinspired Microstructures. *Nat. Commun.* **2013**, *4*, 1712.

(4) Forterre, Y.; Skotheim, J. M.; Dumais, J.; Mahadevan, L. How the Venus Flytrap Snaps. *Nature* **2005**, *433*, 421−425.

(5) Ko, H.; Javey, A. Smart Actuators and Adhesives for Reconfigurable Matter. *Acc. Chem. Res.* **2017**, *50*, 691−702.

(6) Ionov, L. Biomimetic Hydrogel-Based Actuating Systems. *Adv. Funct. Mater.* **2013**, *23*, 4555−4570.

(7) Li, S.; Wang, K. W. Plant-Inspired Adaptive Structures and Materials for Morphing and Actuation: a Review. *Bioinspiration Biomimetics* **2016**, *12*, 011001.

(8) Gracias, D. H. Stimuli Responsive Self-Folding Using Thin Polymer Films. *Curr. Opin. Chem. Eng.* **2013**, *2*, 112−119.

(9) Kempaiah, R.; Nie, Z. From Nature to Synthetic Systems: Shape Transformation in Soft Materials. *J. Mater. Chem. B* **2014**, *2*, 2357−2368.

(10) Ionov, L. Hydrogel-Based Actuators: Possibilities and Limitations. *Mater. Today* **2014**, *17*, 494−503.

(11) van Manen, T.; Janbaz, S.; Zadpoor, A. A. Programming the Shape-Shifting of Flat Soft Matter. *Mater. Today* **2018**, *21*, 144−163.

(12) Liu, Y.; Genzer, J.; Dickey, M. D. " 2D or Not 2D": Shape-Programming Polymer Sheets. *Prog. Polym. Sci.* **2016**, *52*, 79−106.

(13) Jeon, S.-J.; Hauser, A. W.; Hayward, R. C. Shape-Morphing Materials from Stimuli-Responsive Hydrogel Hybrids. *Acc. Chem. Res.* **2017**, *50*, 161−169.

(14) Löwenberg, C.; Balk, M.; Wischke, C.; Behl, M.; Lendlein, A. Shape-Memory Hydrogels: Evolution of Structural Principles To Enable Shape Switching of Hydrophilic Polymer Networks. *Acc. Chem. Res.* **2017**, *50*, 723−732.

(15) de Espinosa, L. M.; Meesorn, W.; Moatsou, D.; Weder, C. Bioinspired Polymer Systems with Stimuli-Responsive Mechanical Properties. *Chem. Rev.* **2017**, *117*, 12851−12892.

(16) Rogers, J.; Huang, Y.; Schmidt, O. G.; Gracias, D. H. Origami MEMS and NEMS. *MRS Bull.* **2016**, *41*, 123−129.

(17) Xu, L.; Shyu, T. C.; Kotov, N. A. Origami and Kirigami Nanocomposites. *ACS Nano* **2017**, *11*, 7587−7599.

(18) Zhao, Q.; Qi, H. J.; Xie, T. Recent Progress in Shape Memory Polymer: New Behavior, Enabling materials, and Mechanistic Understanding. *Prog. Polym. Sci.* **2015**, *49-50*, 79−120.

(19) Zhou, J.; Sheiko, S. S. Reversible Shape-Shifting in Polymeric Materials. *J. Polym. Sci., Part B: Polym. Phys.* **2016**, *54*, 1365−1380.

(20) White, T. J.; Broer, D. J. Programmable and Adaptive Mechanics with Liquid Crystal Polymer Networks and Elastomers. *Nat. Mater.* **2015**, *14*, 1087−1098.
(21) Koerner, H.; White, T. J.; Tabiryan, N. V.; Bunning, T. J.; Vaia, R. A. Photogenerating Work from Polymers. *Mater. Today* **2008**, *11*, 34−42.
(22) Hager, M. D.; Bode, S.; Weber, C.; Schubert, U. S. Shape Memory Polymers: Past, Present and Future Developments. *Prog. Polym. Sci.* **2015**, *49-50*, 3−33.
(23) Han, D.-D.; Zhang, Y.-L.; Ma, J.-N.; Liu, Y.-Q.; Han, B.; Sun, H.-B. Light-Mediated Manufacture and Manipulation of Actuators. *Adv. Mater.* **2016**, *28*, 8328−8343.
(24) Jiang, H. Y.; Kelch, S.; Lendlein, A. Polymers Move in Response to Light. *Adv. Mater.* **2006**, *18*, 1471−1475.
(25) Carpi, F.; Kornbluh, R.; Sommer-Larsen, P.; Alici, G. Electroactive Polymer Actuators as Artificial Muscles: Are They Ready for Bioinspired Applications? *Bioinspiration Biomimetics* **2011**, *6*, 045006.
(26) Studart, A. R.; Erb, R. M. Bioinspired Materials that Self-Shape through Programmed Microstructures. *Soft Matter* **2014**, *10*, 1284−1294.
(27) Ube, T.; Ikeda, T. Photomobile Polymer Materials with Crosslinked Liquid-Crystalline Structures: Molecular Design, Fabrication, and Functions. *Angew. Chem., Int. Ed.* **2014**, *53*, 10290−10299.
(28) Pilate, F.; Toncheva, A.; Dubois, P.; Raquez, J.-M. Shape-Memory Polymers for Multiple Applications in the Materials World. *Eur. Polym. J.* **2016**, *80*, 268−294.
(29) Stoychev, G. V.; Ionov, L. Actuating Fibers: Design and Applications. *ACS Appl. Mater. Interfaces* **2016**, *8*, 24281−24294.
(30) Zhang, Y.; Zhang, F.; Yan, Z.; Ma, Q.; Li, X. L.; Huang, Y. G.; Rogers, J. A. Printing, Folding and Assembly Methods for Forming 3D Mesostructures in Advanced Materials. *Nat. Rev. Mater.* **2017**, *2*, 17019.
(31) Hines, L.; Petersen, K.; Lum, G. Z.; Sitti, M. Soft Actuators for Small-Scale Robotics. *Adv. Mater.* **2017**, *29*, 1603483.
(32) Quiñones, V. A. B.; Zhu, H.; Solovev, A. A.; Mei, Y. F.; Gracias, D. H. Origami Biosystems: 3D Assembly Methods for Biomedical Applications. *Adv. Biosyst.* **2018**, *2*, 1800230.
(33) Xu, W.; Kwok, K. S.; Gracias, D. H. Ultrathin Shape Change Smart Materials. *Acc. Chem. Res.* **2018**, *51*, 436−444.
(34) Momeni, F.; M.Mehdi Hassani.N, S.; Liu, X.; Ni, J. A Review of 4D Printing. *Mater. Des.* **2017**, *122*, 42−79.
(35) Miao, S.; Castro, N.; Nowicki, M.; Xia, L.; Cui, H.; Zhou, X.; Zhu, W.; Lee, S.-j.; Sarkar, K.; Vozzi, G.; Tabata, Y.; Fisher, J.; Zhang, L. G. 4D Printing of Polymeric Materials for Tissue and Organ Regeneration. *Mater. Today* **2017**, *20*, 577−591.
(36) Huang, G.; Mei, Y.; Thurmer, D. J.; Coric, E.; Schmidt, O. G. Rolled-Up Transparent Microtubes as Two-Dimensionally Confined Culture Scaffolds of Individual Yeast Cells. *Lab Chip* **2009**, *9*, 263−268.
(37) Jamal, M.; Bassik, N.; Cho, J.-H.; Randall, C. L.; Gracias, D. H. Directed Growth of Fibroblasts into Three Dimensional Micropatterned Geometries via Self-Assembling Scaffolds. *Biomaterials* **2010**, *31*, 1683−1690.
(38) Cheng, S.; Jin, Y.; Wang, N.; Cao, F.; Zhang, W.; Bai, W.; Zheng, W.; Jiang, X. Self-Adjusting, Polymeric Multilayered Roll that can Keep the Shapes of the Blood Vessel Scaffolds during Biodegradation. *Adv. Mater.* **2017**, *29*, 1700171.
(39) Yuan, B.; Jin, Y.; Sun, Y.; Wang, D.; Sun, J.; Wang, Z.; Zhang, W.; Jiang, X. A Strategy for Depositing Different Types of Cells in Three Dimensions to Mimic Tubular Structures in Tissues. *Adv. Mater.* **2012**, *24*, 890−896.
(40) Gelebart, A. H.; Jan Mulder, D.; Varga, M.; Konya, A.; Vantomme, G.; Meijer, E. W.; Selinger, R. L. B.; Broer, D. J. Making Waves in a Photoactive Polymer Film. *Nature* **2017**, *546*, 632−636.
(41) Lu, X.; Guo, S.; Tong, X.; Xia, H.; Zhao, Y. Tunable Photocontrolled Motions Using Stored Strain Energy in Malleable Azobenzene Liquid Crystalline Polymer Actuators. *Adv. Mater.* **2017**, *29*, 1606467.
(42) Mu, J.; Hou, C.; Wang, H.; Li, Y.; Zhang, Q.; Zhu, M. Origami-Inspired Active Graphene-Based Paper for Programmable Instant Self-Folding Walking Devices. *Sci. Adv.* **2015**, *1*, No. e1500533.
(43) Hawkes, E.; An, B.; Benbernou, N. M.; Tanaka, H.; Kim, S.; Demaine, E. D.; Rus, D.; Wood, R. J. Programmable Matter by Folding. *Proc. Natl. Acad. Sci. U.S.A.* **2010**, *107*, 12441−12445.
(44) Wehner, M.; Truby, R. L.; Fitzgerald, D. J.; Mosadegh, B.; Whitesides, G. M.; Lewis, J. A.; Wood, R. J. An Integrated Design and Fabrication Strategy for Entirely Soft, Autonomous Robots. *Nature* **2016**, *536*, 451−455.
(45) Arazoe, H.; Miyajima, D.; Akaike, K.; Araoka, F.; Sato, E.; Hikima, T.; Kawamoto, M.; Aida, T. An Autonomous Actuator Driven by Fluctuations in Ambient Humidity. *Nat. Mater.* **2016**, *15*, 1084−1089.
(46) Zhang, L.; Liang, H.; Jacob, J.; Naumov, P. Photogated Humidity-Driven Motility. *Nat. Commun.* **2015**, *6*, 7429.
(47) Wie, J. J.; Shankar, M. R.; White, T. J. Photomotility of Polymers. *Nat. Commun.* **2016**, *7*, 13260.
(48) Huang, H.-W.; Sakar, M. S.; Petruska, A. J.; Pane, S.; Nelson, B. J. Soft Micromachines with Programmable Motility and Morphology. *Nat. Commun.* **2016**, *7*, 12263.
(49) Guin, T.; Settle, M. J.; Kowalski, B. A.; Auguste, A. D.; Beblo, R. V.; Reich, G. W.; White, T. J. Layered Liquid Crystal Elastomer Actuators. *Nat. Commun.* **2018**, *9*, 2531.
(50) Iamsaard, S.; Asshoff, S. J.; Matt, B.; Kudernac, T.; Cornelissen, J. J. L. M.; Fletcher, S. P.; Katsonis, N. Conversion of Light into Macroscopic Helical Motion. *Nat. Chem.* **2014**, *6*, 229−235.
(51) Malachowski, K.; Jamal, M.; Jin, Q.; Polat, B.; Morris, C. J.; Gracias, D. H. Self-Folding Single Cell Grippers. *Nano Lett.* **2014**, *14*, 4164−4170.
(52) Breger, J. C.; Yoon, C.; Xiao, R.; Kwag, H. R.; Wang, M. O.; Fisher, J. P.; Nguyen, T. D.; Gracias, D. H. Self-Folding Thermo-Magnetically Responsive Soft Microgrippers. *ACS Appl. Mater. Interfaces* **2015**, *7*, 3398−3405.
(53) Jamal, M.; Zarafshar, A. M.; Gracias, D. H. Differentially Photo-Crosslinked Polymers Enable Self-Assembling Microfluidics. *Nat. Commun.* **2011**, *2*, 527.
(54) Lv, J.-a.; Liu, Y.; Wei, J.; Chen, E.; Qin, L.; Yu, Y. Photocontrol of Fluid Slugs in Liquid Crystal Polymer Microactuators. *Nature* **2016**, *537*, 179−184.
(55) Shim, T. S.; Kim, S.-H.; Heo, C.-J.; Jeon, H. C.; Yang, S.-M. Controlled Origami Folding of Hydrogel Bilayers with Sustained Reversibility for Robust Microcarriers. *Angew. Chem., Int. Ed.* **2012**, *51*, 1420−1423.
(56) Malachowski, K.; Breger, J.; Kwag, H. R.; Wang, M. O.; Fisher, J. P.; Selaru, F. M.; Gracias, D. H. Stimuli-Responsive Theragrippers for Chemomechanical Controlled Release. *Angew. Chem., Int. Ed.* **2014**, *53*, 8045−8049.
(57) Magdanz, V.; Guix, M.; Hebenstreit, F.; Schmidt, O. G. Dynamic Polymeric Microtubes for the Remote-Controlled Capture, Guidance, and Release of Sperm Cells. *Adv. Mater.* **2016**, *28*, 4084−4089.
(58) Ye, C.; Tsukruk, V. V. Designing Two-Dimensional Materials that Spring Rapidly into Three-Dimensional Shapes. *Science* **2015**, *347*, 130−131.
(59) Silverberg, J. L.; Evans, A. A.; McLeod, L.; Hayward, R. C.; Hull, T.; Santangelo, C. D.; Cohen, I. Using Origami Design Principles to Fold Reprogrammable Mechanical Metamaterials. *Science* **2014**, *345*, 647−650.
(60) Liu, J.; Erol, O.; Pantula, A.; Liu, W.; Jiang, Z.; Kobayashi, K.; Chatterjee, D.; Hibino, N.; Romer, L. H.; Kang, S. H.; Nguyen, T. D.; Gracias, D. H. Dual-Gel 4D Printing of Bioinspired Tubes. *ACS Appl. Mater. Interfaces* **2019**, *11*, 8492−8498.
(61) Käpylä, E.; Delgado, S. M.; Kasko, A. M. Shape-Changing Photodegradable Hydrogels for Dynamic 3D Cell Culture. *ACS Appl. Mater. Interfaces* **2016**, *8*, 17885−17893.

https://dx.doi.org/10.1021/acsami.9b23195
ACS Appl. Mater. Interfaces 2020, 12, 13521−13528

(62) Qian, X.; Chen, Q.; Yang, Y.; Xu, Y.; Li, Z.; Wang, Z.; Wu, Y.; Wei, Y.; Ji, Y. Untethered Recyclable Tubular Actuators with Versatile Locomotion for Soft Continuum Robots. *Adv. Mater.* **2018**, *30*, 1801103.
(63) Baek, K.; Jeong, J. H.; Shkumatov, A.; Bashir, R.; Kong, H. In Situ Self-Folding Assembly of a Multi-Walled Hydrogel Tube for Uniaxial Sustained Molecular Release. *Adv. Mater.* **2013**, *25*, 5568−5573.
(64) Zakharchenko, S.; Puretskiy, N.; Stoychev, G.; Stamm, M.; Ionov, L. Temperature Controlled Encapsulation and Release Using Partially Biodegradable Thermo-Magneto-Sensitive Self-Rolling Tubes. *Soft Matter* **2010**, *6*, 2633−2636.
(65) Xi, W.; Schmidt, C. K.; Sanchez, S.; Gracias, D. H.; Carazo-Salas, R. E.; Butler, R.; Lawrence, N.; Jackson, S. P.; Schmidt, O. G. Molecular Insights into Division of Single Human Cancer Cells in On-Chip Transparent Microtubes. *ACS Nano* **2016**, *10*, 5835−5846.
(66) Stoychev, G.; Zakharchenko, S.; Turcaud, S.; Dunlop, J. W. C.; Ionov, L. Shape-Programmed Folding of Stimuli-Responsive Polymer Bilayers. *ACS Nano* **2012**, *6*, 3925−3934.
(67) Chun, I. S.; Challa, A.; Derickson, B.; Hsia, K. J.; Li, X. Geometry Effect on the Strain-Induced Self-Rolling of Semiconductor Membranes. *Nano Lett.* **2010**, *10*, 3927−3932.
(68) Wang, M.; He, L.; Zorba, S.; Yin, Y. Magnetically Actuated Liquid Crystals. *Nano Lett.* **2014**, *14*, 3966−3971.
(69) Zhao, Z.; Wu, J.; Mu, X.; Chen, H.; Qi, H. J.; Fang, D. Origami by Frontal Photopolymerization. *Sci. Adv.* **2017**, *3*, No. e1602326.
(70) Guo, H.; Liu, Y.; Yang, Y.; Wu, G.; Demella, K.; Raghavan, S. R.; Nie, Z. A Shape-Shifting Composite Hydrogel Sheet with Spatially Patterned Plasmonic Nanoparticles. *J. Mater. Chem. B* **2019**, *7*, 1679−1683.

https://dx.doi.org/10.1021/acsami.9b23195
ACS Appl. Mater. Interfaces 2020, 12, 13521−13528